

Slow Magnetic Relaxation in a Dy₃ Triangle and a Bistriangle Dy₆ Cluster

Wen Wang,^a Tao Shang,^c Juan Wang,^a Bin-Ling Yao^b, Li-Cun Li,^a Yue Ma,*^a Qing-Lun Wang,^a Yuan-Zhu Zhang,^{*b} Yi-Quan Zhang,^{*c} and Bin Zhao^a

Crystal Data and Structures

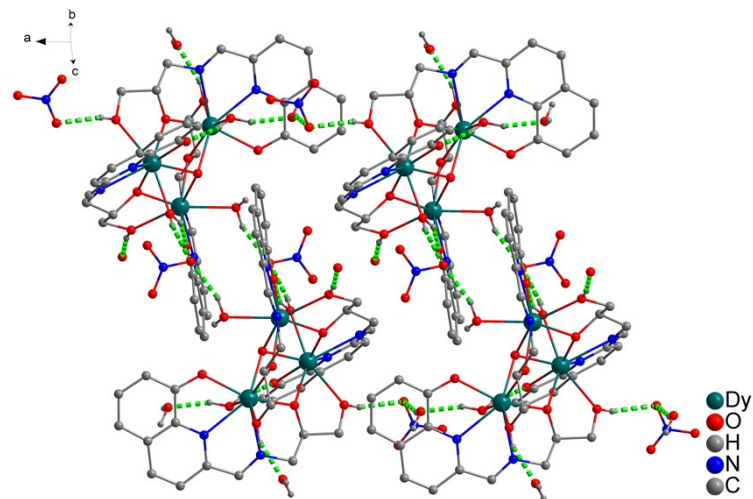


Fig. S1. Packing diagram of complex 1 along *a* axis. The green dashed line indicates the intramolecular hydrogen bond.

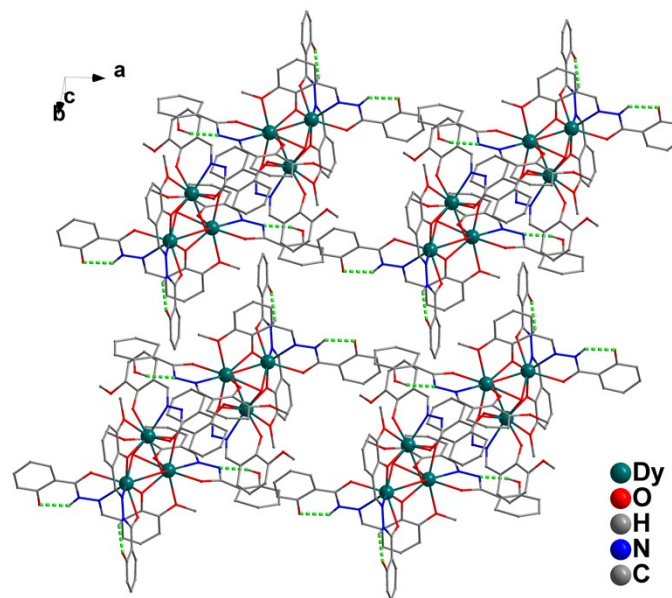


Fig. S2. Packing diagram of complex 2 along *b* axis. The green dashed line indicates the intramolecular hydrogen bond.

Table S1. Dy^{III} Geometry Analysis by Using the SHAPE Software for **1**.

Dy ^{III}	D _{2d} -TDD-8	C _{2v} - BTPR-8	C _{2v} - JBTPR-8
Dy1	1.999	2.269	2.917
Dy2	2.027	2.255	2.867
Dy3	2.245	1.832	2.592

TDD-8 = Triangular dodecahedron; BTPR-8 = Biaugmented trigonal prism; JBTPR-8 = Biaugmented trigonal prism J50.

Table S2. Dy^{III} Geometry Analysis by Using the SHAPE Software for **2**.

Dy ^{III}	D _{2d} -TDD-8	C _{2v} - BTPR-8	C _{2v} - JBTPR-8
Dy1	2.902	2.579	2.372
Dy2	3.243	4.237	3.955
Dy3	3.326	1.805	2.726

TDD-8 = Triangular dodecahedron; BTPR-8 = Biaugmented trigonal prism; JBTPR-8 = Biaugmented trigonal prism J50.

Table S3. Selected bond lengths [Å] and angles [°] for **1**.

Bond Lengths			
Dy1-O6	2.268(5)	Dy2-O11	2.420(7)
Dy1-O9	2.319(5)	Dy2-O7	2.425(6)
Dy1-O5	2.322(5)	Dy2-N1	2.466(7)
Dy1-O1	2.366(5)	Dy2-N2	2.526(7)
Dy1-O12	2.426(5)	Dy2-Dy3	3.7305(7)
Dy1-O10	2.438(6)	Dy3-O9	2.256(6)
Dy1-N5	2.466(6)	Dy3-O8	2.303(7)
Dy1-N6	2.486(7)	Dy3-O3	2.309(5)
Dy1-Dy3	3.7550(6)	Dy3-O1	2.362(5)
Dy1-Dy2	3.7814(8)	Dy3-N3	2.447(7)
Dy2-O3	2.277(5)	Dy3-O13	2.457(6)
Dy2-O2	2.283(5)	Dy3-O4	2.459(6)
Dy2-O6	2.310(6)	Dy3-N4	2.490(8)
Dy2-O1	2.378(5)		
Bond angles			
O6-Dy1-O9	89.46(18)	O11-Dy2-O7	146.5(2)
O6-Dy1-O5	158.5(2)	O3-Dy2-N1	128.5(2)
O9-Dy1-O5	85.82(18)	O2-Dy2-N1	67.1(2)
O6-Dy1-O1	71.56(19)	O6-Dy2-N1	128.7(2)
O9-Dy1-O1	71.22(19)	O1-Dy2-N1	141.5(2)
O5-Dy1-O1	87.05(19)	O11-Dy2-N1	77.0(2)
O6-Dy1-O12	82.85(19)	O7-Dy2-N1	73.5(2)

O9-Dy1-O12	144.6(2)	O3-Dy2-N2	67.0(2)
O5-Dy1-O12	88.89(19)	O2-Dy2-N2	130.3(2)
O1-Dy1-O12	73.57(18)	O6-Dy2-N2	129.4(2)
O6-Dy1-O10	104.2(2)	O1-Dy2-N2	135.7(2)
O9-Dy1-O10	65.9(2)	O11-Dy2-N2	77.7(2)
O5-Dy1-O10	93.0(2)	O7-Dy2-N2	75.1(2)
O1-Dy1-O10	136.99(18)	N1-Dy2-N2	63.2(2)
O12-Dy1-O10	149.43(19)	O9-Dy3-O8	151.9(2)
O6-Dy1-N5	128.8(2)	O9-Dy3-O3	92.8(2)
O9-Dy1-N5	133.51(19)	O8-Dy3-O3	89.1(2)
O5-Dy1-N5	66.9(2)	O9-Dy3-O1	72.37(19)
O1-Dy1-N5	138.8(2)	O8-Dy3-O1	81.4(2)
O12-Dy1-N5	74.54(19)	O3-Dy3-O1	73.31(18)
O10-Dy1-N5	78.2(2)	O9-Dy3-N3	128.1(2)
O6-Dy1-N6	68.0(2)	O8-Dy3-N3	68.0(3)
O9-Dy1-N6	128.4(2)	O3-Dy3-N3	130.1(2)
O5-Dy1-N6	130.1(2)	O1-Dy3-N3	139.1(2)
O1-Dy1-N6	133.8(2)	O9-Dy3-O13	79.5(2)
O12-Dy1-N6	80.2(2)	O8-Dy3-O13	85.6(2)
O10-Dy1-N6	75.4(2)	O3-Dy3-O13	151.45(19)
N5-Dy1-N6	63.2(2)	O1-Dy3-O13	78.16(19)
O3-Dy2-O2	158.89(19)	N3-Dy3-O13	73.1(2)
O3-Dy2-O6	93.0(2)	O9-Dy3-O4	111.1(2)
O2-Dy2-O6	83.53(19)	O8-Dy3-O4	95.3(2)

O3-Dy2-O1	73.60(18)	O3-Dy3-O4	65.77(19)
O2-Dy2-O1	85.66(19)	O1-Dy3-O4	139.00(19)
O6-Dy2-O1	70.65(19)	N3-Dy3-O4	72.7(2)
O3-Dy2-O11	80.7(2)	O13-Dy3-O4	142.64(19)
O2-Dy2-O11	91.0(2)	O9-Dy3-N4	67.9(2)
O6-Dy2-O11	147.2(2)	O8-Dy3-N4	132.2(2)
O1-Dy2-O11	76.7(2)	O3-Dy3-N4	123.8(2)
O3-Dy2-O7	105.7(2)	O1-Dy3-N4	136.9(2)
O2-Dy2-O7	91.9(2)	N3-Dy3-N4	64.3(3)
O6-Dy2-O7	66.21(19)	O13-Dy3-N4	78.9(2)
O1-Dy2-O7	136.78(19)	O4-Dy3-N4	73.1(2)

Table S4. Hydrogen bond lengths [Å] and angles [°] for **1**.

D-H···A	<i>d</i> (D-H)	<i>d</i> (H···A)	<i>d</i> (D···A)	\angle (DHA)
O12-H12a···O6	0.8800	1.8000	2.646(7)	161.00
O12-H12b···O6	0.8900	1.8100	2.675(4)	162.00
O9-H9···O21	0.8600	1.8800	2.704(6)	160.00
O7-H7···O18a	0.7300	2.0800	2.794(7)	165.00
O5-H5···O20	0.8500	1.8500	2.699(6)	172.00
O11-H11a···O15	0.8500	2.1100	2.922(5)	158.00
O11-H11b···O10	0.8700	1.8500	2.662(4)	156.00
O13-H13a···O15	0.8500	1.9800	2.799(6)	161.00
O22-H22a···O18a	0.8500	1.9700	2.794(3)	162.00

Table S5. Selected bond lengths [Å] and angles [°] for **2**.

Bond Lengths			
Dy1-O1	2.575(10)	Dy2-O8	2.369(10)
Dy1-O2	2.093(9)	Dy2-O12	2.371(10)
Dy1-O3	2.182(9)	Dy2-N3	2.432(12)
Dy1-O5	2.244(10)	Dy2-N6	2.359(13)
Dy1-O6	2.667(11)	Dy3-O1	2.238(9)
Dy1-O7	2.372(10)	Dy3-O2	2.802(11)
Dy1-N2	2.413(10)	Dy3-O12	2.344(10)
Dy1-O4#1	2.546(10)	Dy3-O13	2.579(10)
Dy2-O1	2.475(10)	Dy3-O16	2.113(10)
Dy2-O2	2.364(9)	Dy3-O14	2.393(13)
Dy2-O7	2.204(9)	Dy3-N7	2.665(14)
Dy2-O10	2.536(12)	Dy3-O4#1	2.288(9)
Bond angles			
O1-Dy1-O6	132.6(3)	O8-Dy2-O10	121.4(4)
O2-Dy1-O1	63.7(3)	O8-Dy2-O12	72.0(4)
O2-Dy1-O3	136.2(4)	O8-Dy2-N3	65.4(4)
O2-Dy1-O5	88.9(4)	O12-Dy2-O1	65.6(3)
O2-Dy1-O6	114.2(4)	O12-Dy2-O10	134.3(4)
O2-Dy1-O7	75.5(3)	O12-Dy2-N3	137.1(4)
O2-Dy1-N2	148.3(3)	N3-Dy2-O1	108.0(4)
O2-Dy1-O4#1	81.0(4)	N3-Dy2-O10	76.2(5)
O3-Dy1-O1	73.6(3)	N6-Dy2-O1	146.5(4)

O3-Dy1-O5	134.9(3)	N6-Dy2-O2	106.8(4)
O3-Dy1-O6	87.1(4)	N6-Dy2-O10	61.5(4)
O3-Dy1-O7	83.6(4)	N6-Dy2-O8	80.6(4)
O3-Dy1-N2	68.4(3)	N6-Dy2-O12	80.9(4)
O3-Dy1-O4#1	92.1(3)	N6-Dy2-N3	96.9(5)
O5-Dy1-O1	148.4(3)	O1-Dy3-O2	58.2(3)
O5-Dy1-O6	71.4(4)	O1-Dy3-O12	69.9(3)
O5-Dy1-O7	116.4(4)	O1-Dy3-O13	114.7(3)
O5-Dy1-N2	69.5(4)	O1-Dy3-O14	87.1(4)
O5-Dy1-O4#1	94.5(4)	O1-Dy3-N7	140.4(4)
O7-Dy1-O1	73.7(3)	O1-Dy3-O4#1	77.6(3)
O7-Dy1-O6	61.2(3)	O12-Dy3-O2	63.4(3)
O7-Dy1-N2	134.5(3)	O12-Dy3-O13	70.3(4)
O7-Dy1-O4#1	140.2(3)	O12-Dy3-O14	117.5(4)
N2-Dy1-O1	126.7(4)	O12-Dy3-N7	142.6(4)
N2-Dy1-O6	81.6(4)	O13-Dy3-O2	132.5(3)
N2-Dy1-O4#1	78.0(3)	O13-Dy3-N7	75.3(4)
O4#1-Dy1-O1	67.2(3)	O16-Dy3-O1	137.4(4)
O4#1-Dy1-O6	158.3(3)	O16-Dy3-O2	79.2(4)
O1-Dy2-O10	145.5(3)	O16-Dy3-O12	93.6(4)
O2-Dy2-O1	62.1(3)	O16-Dy3-O13	94.3(4)
O2-Dy2-O10	95.2(4)	O16-Dy3-O14	134.0(4)
O2-Dy2-O8	139.9(4)	O16-Dy3-N7	74.8(4)
O2-Dy2-O12	70.5(3)	O16-Dy3-O4#1	89.0(4)

O2-Dy2-N3	147.1(4)	O14-Dy3-O2	143.7(3)
O7-Dy2-O1	78.6(4)	O14-Dy3-O13	68.7(4)
O7-Dy2-O2	73.7(3)	O14-Dy3-N7	59.9(4)
O7-Dy2-O10	69.7(4)	N7-Dy3-O2	143.4(4)
O7-Dy2-O8	131.2(4)	O4#1-Dy3-O2	72.3(3)
O7-Dy2-O12	137.9(4)	O4#1-Dy3-O12	134.2(4)
O7-Dy2-N3	73.6(4)	O4#1-Dy3-O13	155.1(4)
O7-Dy2-N6	131.1(4)	O4#1-Dy3-O14	91.4(4)
O8-Dy2-O1	89.6(4)	O4#1-Dy3-N7	81.8(4)

Symmetry codes: #1 -x+2,-y+2,-z

Table S6. Hydrogen bond lengths [\AA] and angles [$^\circ$] for **2**.

D-H \cdots A	$d(\text{D-H})$	$d(\text{H}\cdots\text{A})$	$d(\text{D}\cdots\text{A})$	$\angle(\text{DHA})$
N5-H5 \cdots O11	0.8800	2.0300	2.644(12)	126.00
N4-H4 \cdots O9	0.8800	1.8700	2.541(10)	131.00
O15-H15 \cdots N8	0.8200	2.0600	2.728(14)	139.00

Magnetic characterization

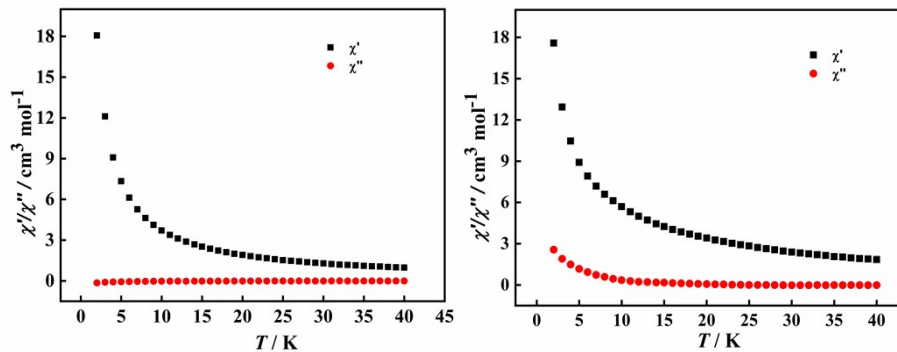


Fig. S3. Temperature dependence of the χ' and χ'' ac magnetic susceptibilities for complexes **1** and **2** in 1000 Hz under zero dc field.

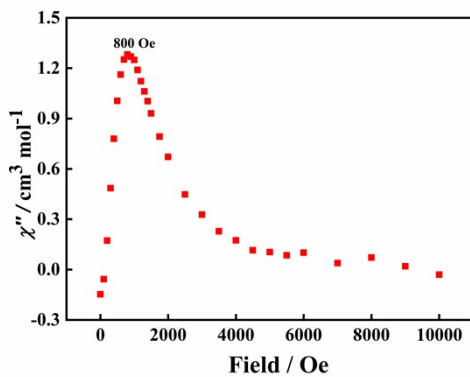


Fig. S4. The field dependence of the χ'' ac magnetic susceptibilities for complex **1** at 1.9 K, 997 Hz.

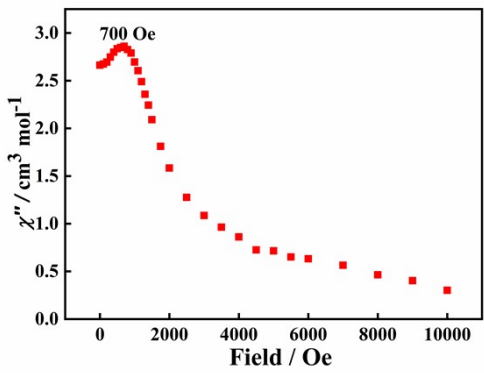


Fig. S5. The field dependence of the χ'' ac magnetic susceptibilities for complex **2** at 1.9 K, 997 Hz.

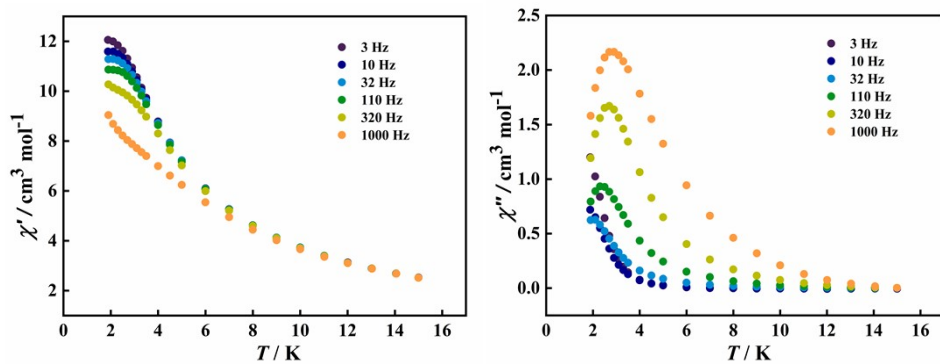


Fig. S6. The temperature dependence of the χ' and χ'' ac magnetic susceptibilities for complex **1** measured under 800 Oe dc field.

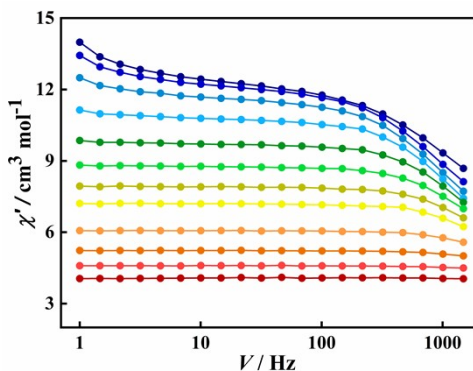


Fig. S7. Frequency dependence of the χ' ac magnetic susceptibilities for complex **1** measured at 1.9-9.0 K under 800 Oe dc field.

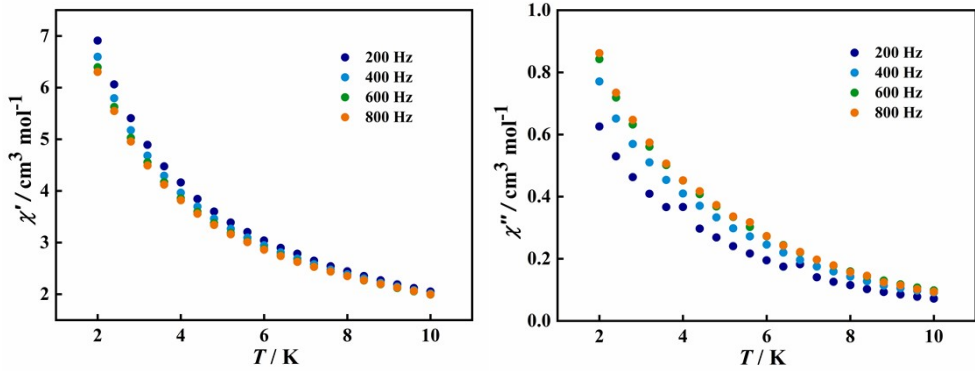


Fig. S8. The temperature dependence of the χ' and χ'' ac magnetic susceptibilities for complex **2** measured under 700 Oe dc field.

Table S7. Fitted parameters α with Debye model under 1.9 K-9.0 K for complexes **1**.

Temperature/K	α_1	α_2
1.9	0.4128	0.2141
2.2	0.4032	0.2032
2.5	0.3222	0.1962
3.0	0.3463	0.1384
3.5	0.2359	0.1198
4.0	0.1033	0.1035
4.5	0.0715	0.0719
5.0	0.0692	0.0357
6.0	0.0292	0.0211
7.0	0.0300	0.0010
8.0	0.0432	0.0010
9.0	0.0100	1.3962E-14

Computational details

Complex **1** has three magnetic center Dy^{III} ions and **2** has six ones. Considering the centrosymmetric structure of complex **2**, we extracted the model structure only including three Dy^{III} ions on the one hand (see Fig. S9). For each of **1** and **2**, three types of **Dy1**, **Dy2** and **Dy3** fragments shown in Figure S1 would be calculated by us to investigate their magnetic properties. Complete-active-space self-consistent field (CASSCF) calculations on three types of individual Dy^{III} fragments for each complex have been carried out with OpenMolcas^{S1} program package. **1_Dy1** **1_Dy2** and **1_Dy3** were calculated respectively keeping the experimentally determined structures of the corresponding compounds while replacing the other Dy^{III} ions with diamagnetic Lu^{III}. In the calculations of **2_Dy1** **2_Dy2** and **2_Dy3**, the nearest Dy^{III} ions were replaced by diamagnetic Lu^{III}, and two Dy^{III} ions on the other side were taken into account by the closed-shell La^{III} ab initio embedding model potentials (AIMP; La.ECP.deGraaf.0s.0s.0e-La-(LaMnO₃).)^{S2}

The basis sets for all atoms are atomic natural orbitals from the ANO-RCC library: ANO-RCC-VTZP for Dy^{III}; VTZ for close N and O; VDZ for distant atoms. The calculations employed the second order Douglas-Kroll-Hess Hamiltonian, where scalar relativistic contractions were taken into account in the basis set and the spin-orbit couplings were handled separately in the restricted active space state interaction (RASSI-SO) procedure.^{S3–S4} For each individual Dy^{III} fragment, active electrons in 7 active orbitals include all *f* electrons (CAS(9 in 7 for Dy^{III})) in the CASSCF calculation. To exclude all the doubts, we calculated all the roots in the active space. We have mixed the maximum number of spin-free state which was possible with our hardware (all from 21 sextets, 128 from 224 quadruplets, 130 from 490 doublets) for each fragment. SINGLE_ANISO^{S5–S7} program was used to obtain the energy levels, **g** tensors, magnetic axes, *et al.* based on the above CASSCF/RASSI-SO calculations.

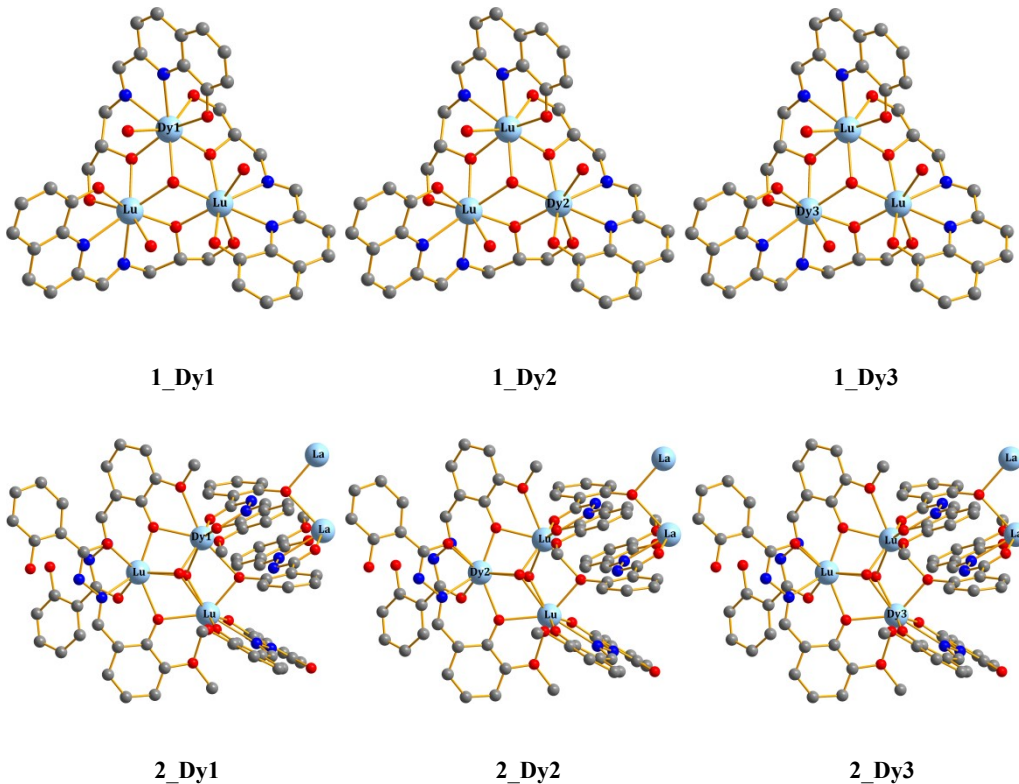


Figure S9. Calculated model structures of individual Dy^{III} fragments of complexes **1** and **2**; H atoms are omitted for clarity.

Table S8. Calculated energy levels (cm^{-1}), \mathbf{g} (g_x , g_y , g_z) tensors of the lowest eight Kramers doublets (KDs) of individual Dy^{III} fragments for complexes **1** and **2** using CASSCF/RASSI-SO with OpenMolcas.

KDs	1_Dy1		1_Dy2		1_Dy3	
	E/cm^{-1}	\mathbf{g}	E/cm^{-1}	\mathbf{g}	E/cm^{-1}	\mathbf{g}
1	0.0	0.007		0.022		0.013
		0.011	0.0	0.031	0.0	0.021
		19.649		19.623		19.628
2	211.3	0.370		0.820		0.554
		1.050	191.9	2.201	190.6	1.849
		16.036		15.265		15.476

		0.529		0.964		0.886
3	268.1	0.692	247.5	1.572	235.7	1.109
		17.966		16.501		17.228
4	416.5	1.054		2.132		1.157
		1.335	378.3	3.277	388.4	1.524
		12.655		11.907		12.838
5	462.2	1.685		0.354		1.410
		3.013	430.0	4.112	438.8	2.938
		13.481		12.112		12.751
6	515.9	4.743		4.459		4.738
		6.354	476.4	6.757	496.1	6.677
		10.440		9.392		10.138
7	607.2	0.419		0.568		0.481
		0.700	569.3	0.860	590.1	0.639
		16.921		16.704		16.863
8	740.2	0.069		0.059		0.087
		0.180	711.0	0.154	700.2	0.233
		19.397		19.444		19.353
KDs	2_Dy1		2_Dy2		2_Dy3	
	E/cm^{-1}	\mathbf{g}	E/cm^{-1}	\mathbf{g}	E/cm^{-1}	\mathbf{g}
1	0.0	0.008		0.031		0.003
		0.015	0.0	0.062	0.0	0.004
		19.744		19.707		19.761

		0.313		0.131		0.076
2	188.6	0.577	67.6	0.234	264.1	0.103
		17.619		17.506		16.906
3	297.9	2.919		2.884		1.153
		5.474	158.0	5.833	448.9	5.615
4	376.1	10.439		13.090		12.415
		7.648		3.125		8.326
		6.494	200.6	4.968	477.2	5.655
5	486.6	1.373		7.912		2.333
		1.659		1.661		3.567
		2.336	250.4	2.873	556.9	4.594
6	581.7	11.503		16.003		12.314
		0.399		8.613		2.657
		0.475	317.9	4.824	604.5	3.396
7	695.3	17.687		0.905		11.094
		0.033		1.968		1.100
		0.149	366.3	5.231	692.7	1.349
8	791.6	17.126		13.592		16.183
		0.038		0.021		0.037
		0.078	569.5	0.029	812.6	0.100
		18.687		19.379		19.629

Table S9. Wave functions with definite projection of the total moment $|m_J\rangle$ for the lowest two KDs of individual Dy^{III} fragments for complexes **1** and **2** using CASSCF/RASSI-SO with OpenMolcas.

	E/cm^{-1}	wave functions				

1_Dy1	0.0	96.3% ±15/2>
	211.3	88.7% ±13/2>+3.5% ±9/2>
	268.1	49.8% ±1/2>+30.0% ±3/2>+10.6% ±5/2>
	416.5	69.1% ±11/2>+7.3% ±9/2>+6.5% ±7/2>+5.7% ±3/2>+5.3% ±5/2>
	462.2	30.7% ±3/2>+27.2% ±5/2>+18.0% ±7/2>+11.1% ±11/2>+6.7% ±1/2>
	515.9	41.4% ±9/2>+18.7% ±7/2>+16.5% ±5/2>+13.8% ±1/2>+4.7% ±3/2>
	607.2	29.5% ±7/2>+24.5% ±9/2>+19.2% ±5/2>+10.4% ±3/2>+9.1% ±1/2>
	740.2	24.7% ±7/2>+19.4% ±5/2>+17.3% ±9/2>+16.6% ±3/2>+14.7% ±1/2>
1_Dy2	0.0	96.1% ±15/2>
	191.9	83.8% ±13/2>+5.1% ±1/2>+3.3% ±5/2>
	247.5	46.7% ±1/2>+29.7% ±3/2>+9.8% ±13/2>+8.9% ±5/2>
	378.3	57.6% ±11/2>+12.4% ±9/2>+8.9% ±5/2>+7.2% ±1/2>+6.6% ±3/2>
	430.0	28.5% ±3/2>+22.3% ±7/2>+20.6% ±5/2>+17.9% ±11/2>+5.4% ±1/2>
	476.4	37.9% ±9/2>+21.6% ±5/2>+20.7% ±7/2>+7.9% ±1/2>+6.2% ±11/2>
	569.3	24.8% ±9/2>+24.7% ±7/2>+17.1% ±5/2>+13.5% ±1/2>+12.0% ±3/2>
	711.0	24.9% ±7/2>+19.6% ±5/2>+17.5% ±9/2>+16.2% ±3/2>+14.2% ±1/2>
1_Dy3	0.0	95.9% ±15/2>
	190.6	84.8% ±13/2>+4.2% ±9/2>+3.9% ±1/2>
	235.7	45.1% ±1/2>+27.9% ±3/2>+12.4% ±5/2>+9.4% ±13/2>
	388.4	67.7% ±11/2>+8.1% ±7/2>+7.5% ±9/2>+5.4% ±3/2>+4.3% ±5/2>
	438.8	27.3% ±3/2>+27.2% ±5/2>+16.6% ±7/2>+12.8% ±11/2>+8.8% ±1/2>
	496.1	42.3% ±9/2>+16.1% ±7/2>+13.6% ±5/2>+13.4% ±1/2>+8.4% ±3/2>
	590.1	29.7% ±7/2>+23.6% ±9/2>+20.4% ±5/2>+10.1% ±3/2>+8.7% ±1/2>
	700.2	24.9% ±7/2>+20.4% ±5/2>+17.8% ±3/2>+15.9% ±1/2>+15.3% ±9/2>

2_Dy1	0.0	98.4% ±15/2>
	188.6	37.3% ±13/2>+17.7% ±9/2>+13.4% ±7/2>+11.3% ±5/2>+11.2% ±11/2>
	297.9	43.7% ±13/2>+14.7% ±7/2>+14.5% ±3/2>+14.4% ±11/2>+7.4% ±1/2>
	376.1	25.6% ±5/2>+23.9% ±11/2>+15.3% ±1/2>+12.8% ±9/2>+10.7% ±13/2>+8.1% ±7/2>
	486.6	27.9% ±11/2>+26.8% ±3/2>+19.9% ±9/2>+11.1% ±1/2>+5.8% ±5/2>
	581.7	47.7% ±1/2>+20.5% ±3/2>+11.4% ±9/2>+9.0% ±7/2>+6.5% ±5/2>
	695.3	27.4% ±7/2>+22.8% ±9/2>+22.2% ±5/2>+12.0% ±11/2>+9.9% ±3/2>
	791.6	24.5% ±5/2>+22.3% ±7/2>+19.4% ±3/2>+13.8% ±9/2>+12.9% ±1/2>
2_Dy2	0.0	97.7% ±15/2>
	67.6	80.1% ±13/2>+17.2% ±11/2>
	158.0	24.5% ±11/2>+20.9% ±9/2>+14.9% ±1/2>+14.5% ±3/2>+10.0% ±5/2>+8.7% ±7/2>
	200.6	26.2% ±11/2>+21.6% ±9/2>+14.5% ±1/2>+10.8% ±3/2>+10.0% ±7/2>+8.8% ±13/2>
	250.4	29.0% ±5/2>+25.3% ±7/2>+18.2% ±3/2>+11.4% ±1/2>+8.0% ±11/2>
	317.9	28.4% ±9/2>+22.1% ±7/2>+18.0% ±1/2>+13.1% ±11/2>+11.9% ±3/2>
	366.3	27.2% ±5/2>+19.1% ±7/2>+18.0% ±3/2>+14.7% ±1/2>+13.8% ±9/2>
	569.5	26.5% ±3/2>+26.0% ±1/2>+22.0% ±5/2>+14.6% ±7/2>+8.0% ±9/2>
2_Dy3	0.0	98.3% ±15/2>
	264.1	95.2% ±13/2>
	448.9	34.5% ±11/2>+27.3% ±1/2>+15.4% ±3/2>+13.6% ±5/2>
	477.2	51.4% ±11/2>+18.8% ±3/2>+16.4% ±1/2>+6.1% ±7/2>
	556.9	26.3% ±9/2>+25.9% ±5/2>+19.7% ±7/2>+11.9% ±3/2>+9.2% ±1/2>
	604.5	49.5% ±9/2>+23.5% ±7/2>+9.8% ±3/2>+9.2% ±5/2>

	692.7	$35.4\% \pm 7/2 > + 25.4\% \pm 5/2 > 13.1\% \pm 3/2 > + 12.2\% \pm 9/2 > + 12.1\% \pm 1/2 >$
	812.6	$33.1\% \pm 1/2 > + 30.9\% \pm 3/2 > + 23.1\% \pm 5/2 > + 10.8\% \pm 7/2 >$

To fit the exchange interactions between Dy^{III} ions in complexes **1** and **2**, we took two steps to obtain them. Firstly, we calculated individual Dy^{III} fragments using CASSCF/RASSI-SO to obtain the corresponding magnetic properties. Then, the exchange interaction between the magnetic centers was considered within the Lines model,^{S8} while the account of the dipole-dipole magnetic coupling is treated exactly. The Lines model is effective and has been successfully used widely in the research field of *d* and *f*-elements single-molecule magnets.^{S9–S10}

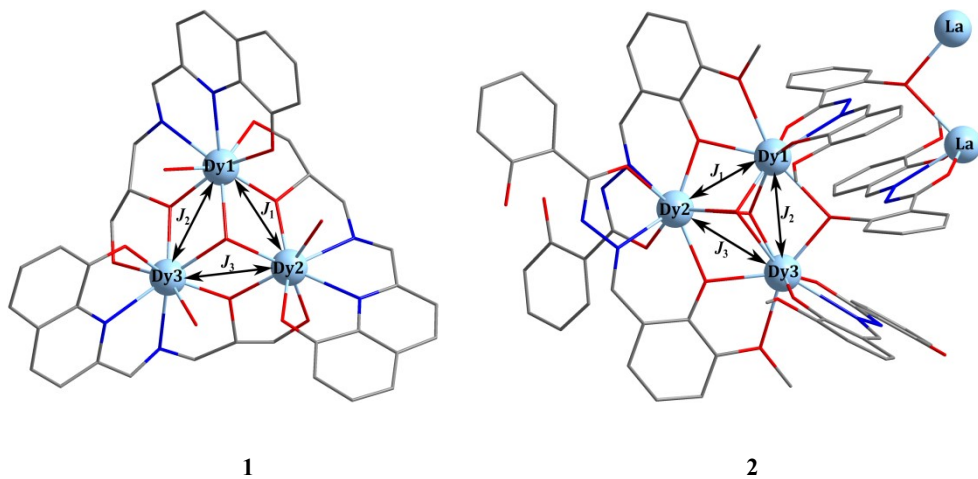


Figure S10. Scheme of the Dy^{III}-Dy^{III} interactions in complexes **1** and **2**.

The Ising exchange Hamiltonian for **1** and **2** is:

$$\hat{H}_{exch} = -J_1 \hat{S}_{Dy1} \hat{S}_{Dy2} - J_2 \hat{S}_{Dy1} \hat{S}_{Dy3} - J_3 \hat{S}_{Dy2} \hat{S}_{Dy3} \quad (\text{S1})$$

The $J_1 = 25 \cos \varphi J_1$, where φ is the angle between the anisotropy axes on sites Dy1 and Dy2, and J_1 is the Lines exchange coupling parameter. The other two interactions J_2 and J_3 also have similar expressions. The $\frac{1}{2}$ is the ground pseudospin on the Dy^{III} site. The total J_{total} is the parameter of the total magnetic interaction (

$\mathcal{J}_{total} = \mathcal{J}_{dipolar} + \mathcal{J}_{exchange}$) between magnetic center ions. The dipolar magnetic couplings can be calculated exactly, while the Lines exchange coupling constants were fitted through comparison of the computed and measured magnetic susceptibilities using the POLY_ANISO program.^{S5-S7}

Table S10. Exchange energies E (cm^{-1}), the transversal magnetic moments Δ_t (μ_B) and the main values of the g_z for the lowest four exchange doublets of complexes **1** and **2**.

	1			2		
exchange doublets	E	Δ_t	g_z	E	Δ_t	g_z
1	0.000000000000	1.883×10^{-5}	33.253	0.000000000000	7.095×10^{-7}	22.885
	0.000000000000			0.000000000001		
2	0.749731966952	7.809×10^{-4}	33.692	0.105473387695	3.036×10^{-6}	27.102
	0.749731966952			0.105473387695		
3	1.156329769108	4.046×10^{-2}	34.067	3.967808456075	5.608×10^{-7}	34.085
	1.156329769108			3.967808456076		
4	1.207341178666	3.076×10^{-2}	33.893	5.321243172509	4.841×10^{-8}	47.477
	1.207341178666			5.321243172510		

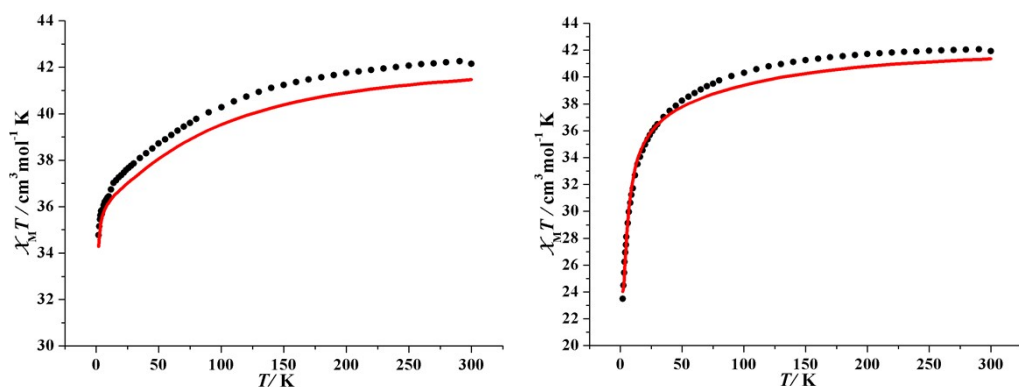


Figure S11. Calculated (red solid line) and experimental (black circle dot) data of magnetic susceptibilities of complexes **1** and **2**. The intermolecular interaction parameters zJ' of **1** and **2** were fitted to -0.01 and 0.08 cm^{-1} , respectively.

1_Dy1	1_Dy2	1_Dy3	2_Dy1	2_Dy2	2_Dy3
Tilted angle between anisotropy axis and the tangential direction($^{\circ}$)					
33.20	26.75	22.07	80.32	0.53	26.75
Tilted angle between anisotropy axis and the Dy_3 plane($^{\circ}$)					
36.35	39.07	35.58	85.63	2.15	69.19

Table S11. Selected angle with anisotropic axis of complexes **1** and **2**.

References:

- S1 F. Aquilante, J. Autschbach, R. K. Carlson, L. F. Chibotaru, M. G. Delcey, L. De Vico, I. F. Galván, N. Ferré, L. M. Frutos, L. Gagliardi, M. Garavelli, A. Giussani, C. E. Hoyer, G. Li Manni, H. Lischka, D. Ma, P. Å. Malmqvist, T. Müller, A. Nenov, M. Olivucci, T. B. Pedersen, D. Peng, F. Plasser, B. Pritchard, M. Reiher, I. Rivalta, I. Schapiro, J. Segarra-Martí, M. Stenrup, D. G. Truhlar, L. Ungur, A. Valentini, S. Vancoillie, V. Veryazov, V. P. Vysotskiy, O. Weingart, F. Zapata and R. Lindh, *J. Comput. Chem.* 2016, **37**, 506–541.
- S2 L. Seijo, Z. Barandiarán, *Computational Chemistry: Reviews of Current Trends*; World Scientific, Inc.: Singapore, 1999; pp 455.
- S3 P. Å. Malmqvist, B. O. Roos, B. Schimmelpfennig, *Chem. Phys. Lett.*, 2002, **357**, 230–240.
- S4 B. A. Heß, C. M. Marian, U. Wahlgren, O. Gropen, *Chem. Phys. Lett.*, 1996, **251**, 365–371.
- S5 L. F. Chibotaru, L. Ungur, A. Soncini, *Angew. Chem., Int. Ed.* 2008, **47**, 4126–4129.
- S6 L. Ungur, W. Van den Heuvel, L. F. Chibotaru, *New J. Chem.* 2009, **33**, 1224–1230.

- S7 L. F. Chibotaru, L. Ungur, C. Aronica, H. Elmoll, G. Pilet, D. Luneau, *J. Am. Chem. Soc.* 2008, **130**, 12445–12455.
- S8 M. E. Lines, *J. Chem. Phys.* 1971, **55**, 2977–2984.
- S9 K. C. Mondal, A. Sundt, Y. H. Lan, G. E. Kostakis, O. Waldmann, L. Ungur, L. F. Chibotaru, C. E. Anson, A. K. Powell, *Angew. Chem., Int. Ed.* 2012, **51**, 7550–7554.
- S10 Langley, S. K.; Wielechowski, D. P.; Vieru, V.; Chilton, N. F.; Moubaraki, B.; Abrahams, B. F.; Chibotaru, L. F.; Murray, K. S. *Angew. Chem., Int. Ed.* **2013**, *52*, 12014–12019.